ISSN 2411-3336; e-ISSN 2541-9404

JOURNAL OF MINING INSTITUTE
Zapiski Gornogo Instituta
Journal homepage: pmi.spmi.ru



Research article
UDC 553.068.3

Indicator role of rare and rare-earth elements of the Northwest manganese ore occurrence (South Africa) in the genetic model of supergene manganese deposits

Aleksandr N. EVDOKIMOV, Benedict L. PHAROE ✉
Saint Petersburg Mining University, Saint Petersburg, Russia

***How to cite this article*:** Evdokimov A.N., Pharoe B.L. Indicator role of rare and rare-earth elements of the Northwest manganese ore occurrence (South Africa) in the genetic model of supergene manganese deposits. Journal of Mining Institute. 2021. Vol. 252, p. 814-825. DOI: 10.31897/PMI.2021.6.4

Abstract. The authors analyzed the content of a number of rare and rare-earth elements in the rocks of the Northwest manganese ore occurrence, confined to the Neoarchean dolomites of the Malmani series of the Transvaal Basin. 30 samples of manganese ores and host rocks were analyzed by ICP-MS and XRF methods. Average values of Post-Archean Australian Shale (PAAS) were used as the geochemical standard for data calculation and normalization. The concentrations of elements normalized on PAAS reveal the LREE anomaly in manganese ores. Positive Ce and negative Y–anomalies indicate the hydro-genetical type of sedimentation of ore minerals from manganese-bearing aqueous solutions. This is consistent with the ratios of the elements: Ce and Y $_{SN}$/Ho $_{SN}$, Ce and Nd, Fe – Mn – (Co + Ni + Cu) × 10. A clear correlation between the contents of rare-earth elements in manganese nodules and the underlying Malmani dolomites indicates their close genetic relationship. Negative Ce and positive Y–anomalies in manganese wad minerals indicate differences in the conditions of their formation. The manganese wad formed earlier than the rest of the ore with the active participation of microorganisms.

***Key words*:** manganese; supergene mineralization; rare-earth elements; weathering crust; South Africa

***Accepted*: 30.11.2021** ***Online*: 09.02.2022** ***Published*: 27.12.2021**

Introduction. A number of classification schemes for manganese deposits are known to determine the nature of manganese deposits and their genesis in various geological conditions [22, 24, 28]. Most of them are usually formed in marine and lacustrine environments [35, 36, 41]. Recently there has been renewed interest in the study of manganese nodules and crusts found in various geological settings. They are also known as polymetallic nodules and crusts. In addition to the extraction of manganese, the possibility of extracting such impurity metals as Ni, Cu, Co, V, and some rare-earth elements from ore aroused interest in the exploration of these deposits.

Areas containing ferromanganese nodules and crusts include the North Pacific Ocean east of Hawaii and the Kiribati Islands: Clarion-Clipperton Zone (CCZ), Cook Islands Exclusive Economic Zone (EEZ), South China Sea (SCS), French Exclusive Economic Zone zone (EEZ), the Wallis and Futuna section (southwestern Pacific), and the Chagos Archipelago in the Central Indian Basin [5, 13, 14, 34].

In the literature, it is customary to divide the deposits of ferromanganese nodules and crusts into three categories according to their genesis: hydrogenic, diagenetic, and hydrothermal [8, 12, 17]. Several scientists [12, 17, 20] have compiled and improved schemes for genetic classifications of

The article is published in open access under the CC BY 4.0 license

these deposits. They described potential sources of ore substances that formed manganese nodules in the lacustrine and oceanic water columns. Manganese nodules and crusts are often enriched in several rare (RE) and rare-earth elements (REE) [22, 28, 41]. In this regard, many authors drew attention to the variability of the contents of rare-earth and rare elements and used this feature to develop genetic schemes of ore formation [4, 29, 44], which help to determine the probable ore source. In particular, the RE and REE contents were taken into account to determine the genesis of oceanic ferromanganese nodules and crusts under various oceanic conditions [2, 3, 24].

Rare and rare-earth elements are often used to determine the conditions for the accumulation of a particular ore type, so an important factor in the accuracy of their diagnosis is the choice of appropriate standards. In the absence of modern and well-founded ideas about the formation of manganese ores in the Malmani area, the authors performed field and analytical work on the area of distribution and vertical sections of the Northwest mineralization (Fig.1). It was taken into account that valid reference standards of these elements are needed for a more reliable analysis of ore matter formed in supergenic zones of ancient manganese rocks. Therefore, in this paper, the authors tried to perform and present the results of the study of the geochemistry of rare and rare-earth elements in manganese ores and host carbonate rocks.

Research method. To complete this work, in 2018-2019 B.L.Pharoe collected manganese ore and host rocks samples at an ore occurrence in the Heifeld region of the Northwest province of South Africa. Samples were taken from a rectangular exploration network consisting of 70 pits located 200 m apart. Samples were collected during the first and second stages of exploration performed by General Nice Manganese Limited. Underlying Neoarchean manganese dolomites and overlying ores (manganese wad and manganese nodules and crusts) were sampled by trenching.

During the first stage of the study, 30 samples were taken from five exploration pits. XRF, ICP-MS, and Powder XRD were used to characterize the chemical and mineralogical composition of the ores. Rare elements were determined using XRF MagiX Fast spectrometer. Analyzes of 31 elements in 22 ore samples were performed on a PerkinElmer NexiON 300X inductively coupled plasma quadrupole mass spectrometer at the University of Johannesburg (table). The data obtained show anomalous concentrations of rare-earth elements, which were then normalized to compositions of the Post-Archean Australian shale [39]. The obtained analytical results made it possible to calculate the correlation coefficients, the ratios between the contents of manganese, rare and rare-earth elements, and also to establish anomalous concentrations of elements – genetic markers of the source of ore manganese.

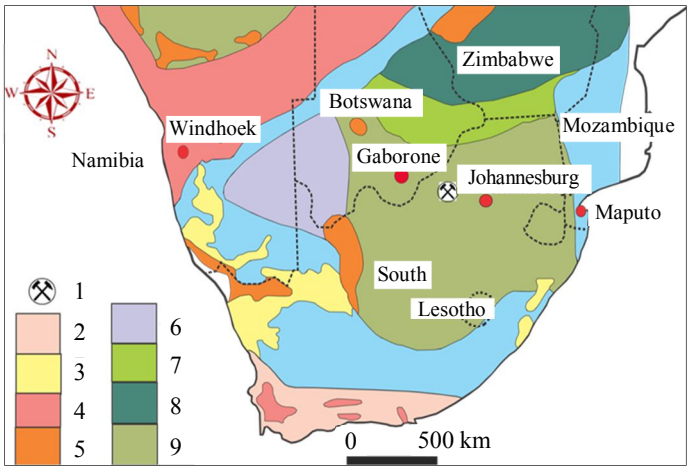


Fig.1. Geological structure of South Africa [16]

1 – area of the Northwest ore occurrence; 2 – quartz arenites, greywackes, shales, siltstones of the Cape Supergroup (P_2); 3 – metasedimentary rocks, granites of the Kibaran orogeny (R_2); 4 – Neoproterozoic Pan-African metamorphic orogenic (amphibolites, granulites, charnockites Neoproterozoic Pan-African orogenic metamorphic (amphibolites, granulites, charnockite (PR_2); 5 – gneisses and granites, formed during the Ubendian orogeny (PR_1^2); 6 – granite, gneisses, rhyolite, and mylonites of the Renoboth craton (PR_1); 7 – granites, greenstone formation, carbonatites, granulites, metagabbro of the Limpopo belt (Ar_2); 8 – granite, gneiss and greenstone complexes of the Zimbabwe craton (Ar_1); 9 – granite, gneiss and greenstone complexes, carbonatites, komatiites of the Kaapvaal craton (Ar_1)

The article is published in open access under the CC BY 4.0 license

Journal of Mining Institute. 2021. Vol. 252. P. 814-825
© Aleksandr N. Evdokimov, Benedict L. Pharoe, 2021

DOI: 10.31897/PMI.2021.6.4

The article is published in open access under the CC BY 4.0 license

Rare-earth element composition of the Northwest Manganese Ore Occurrence, ICP-MS analysis results, ppm

Sample number	La	Ce	Pr	Nd	Sm	Eu	Gd	Tb	Dy	Y	Ho	Er	Tm	Yb	Lu	Sc	V	$(Ce/Ce^*)_{SN}$	$(Eu/Eu^*)_{SN}$	$(La/Yb)_{SN}$	$(Y/Ho)_{SN}$
BH1-C	263.34	758.35	55.35	196.48	37.74	8.74	34.05	4.638	24.23	82.23	4.30	11.08	1.71	11.20	1.63	57.91	315.86				
BH1-D	209.89	639.47	47.23	168.77	32.72	7.65	28.55	3.997	20.52	65.09	3.62	9.23	1.45	9.55	1.36	53.435	318.35	1.50	1.17	1.62	8.57
BH1-E	71.91	490.34	15.92	55.66	10.79	2.60	9.61	1.347	7.22	23.08	1.28	3.36	0.55	3.69	0.55	31.435	245.05	3.33	1.19	1.44	8.61
BH1-F	300.53	639.38	58.47	205.66	38.50	8.90	34.82	4.788	24.79	85.03	4.3	11.30	1.72	11.17	1.66	54.647	289.22	1.19	1.13	1.98	9.42
BH1-G	240.84	658.19	53.50	192.69	36.86	8.52	32.75	4.541	23.63	76.57	4.17	10.58	1.64	10.79	1.57	56.244	320.27	1.37	1.14	1.64	8.74
BH2-C	200.28	734.34	49.09	177.05	35.14	8.21	29.24	4.136	20.93	59.07	3.57	9.01	1.40	9.12	1.31	59.218	354.37	1.67	1.19	1.62	7.88
BH2-D	132.77	425.44	31.43	113.82	22.28	5.24	19.08	2.673	13.77	44.68	2.37	6.17	0.95	6.15	0.89	46.066	263.22	1.52	1.18	1.59	9.00
BH2-E	179.53	400.91	39.85	145.19	27.90	6.48	25.58	3.571	18.65	65.38	3.35	8.57	1.33	8.74	1.24	39.16	243.27	1.13	1.13	1.51	9.29
BH2-F	159.18	437.63	33.38	121.21	22.91	5.48	21.78	2.99	15.63	70.68	2.88	7.54	1.15	7.47	1.11	43.436	273.55	1.47	1.14	1.57	11.67
BH2-G	233.92	693.33	47.33	168.75	32.51	7.72	30.43	4.15	21.80	97.53	3.94	10.30	1.58	10.25	1.55	60.191	421.72	1.62	1.14	1.68	11.78
BH3-C	232.09	775.83	54.94	197.14	39.01	9.18	32.32	4.55	23.20	65.03	3.92	10.06	1.57	10.38	1.50	65.641	424.16	1.57	1.21	1.65	7.90
BH3-D	182.61	613.26	42.96	153.43	30.29	7.10	25.46	3.54	18.05	51.50	3.09	7.95	1.24	8.17	1.18	51.373	317.55	1.58	1.19	1.65	7.94
BH3-E	273.87	978.77	64.82	228.61	45.82	10.62	37.95	5.41	27.38	77.20	4.68	12.12	1.89	12.43	1.80	74.71	394.36	1.65	1.19	1.62	7.86
BH3-F	251.76	933.00	60.02	212.35	43.09	10.03	36.32	5.09	26.06	72.95	4.52	11.43	1.76	11.79	1.72	69.51	346.21	1.70	1.18	1.57	7.68
BH4-D	202.58	640.70	48.20	172.29	34.08	8.01	28.09	3.87	19.62	54.44	3.32	8.41	1.29	8.49	1.21	52.59	429.46	1.47	1.21	1.76	7.81
BH4-E	239.88	801.12	57.67	203.42	40.32	9.50	33.09	4.55	22.67	61.49	3.79	9.54	1.45	9.59	1.37	54.41	642.63	1.52	1.21	1.84	7.72
BH4-F	253.67	709.78	57.76	207.16	39.56	9.17	33.56	4.57	22.99	67.77	3.92	9.93	1.53	9.78	1.41	49.81	545.56	1.36	1.17	1.91	8.24
BH4-G	227.65	626.51	52.33	188.73	36.73	8.46	31.15	4.34	22.14	63.99	3.79	9.70	1.50	9.84	1.42	50.01	373.42	1.34	1.17	1.70	8.04
WAD	22.91	30.16	4.48	17.06	3.24	0.85	3.42	0.47	2.73	27.40	0.57	1.59	0.25	1.53	0.26	10.96	162.79	0.79	1.18	1.10	22.97
GNR DD	86.01	381.48	22.35	79.51	16	3.69	12.42	1.77	8.78	24.24	1.50	3.84	0.60	3.93	0.56	20.92	410.55	1.88	1.22	1.61	7.68
DOL	56.89	129.71	13.51	51.40	9.96	2.23	8.63	1.22	6.27	22.89	1.12	2.85	0.43	2.83	0.43	10.77	72.08	1.13	1.12	1.48	9.70
B3-D	238.66	870.36	56.81	203.09	40.64	9.50	33.83	4.73	24.08	68.83	4.09	10.45	1.63	10.82	1.55	66.81	381.66	1.69	1.19	1.63	8.01

Ce $\left(\frac{Ce_{SN}}{Ce^{*}_{SN}}\right)$ and Eu $\left(\frac{Eu_{SN}}{Eu^{*}_{SN}}\right)$ anomalies were calculated as coefficients normalized to the composition of the Post-Archean Australian clay shale PAAS (SN index) [39] by interpolating the contents of neighboring REE (*) as follows:

$$Ce^{*}_{SN} = 0.5La_{SN} + 0.5Pr_{SN} \quad [17]; \tag{1}$$

$$\frac{Ce_{SN}}{Ce^{*}_{SN}} = \frac{2[Ce]_{SN}}{[Sm]_{SN} + [Pr]_{SN}}; \tag{2}$$

$$\frac{Eu_{SN}}{Eu^{*}_{SN}} = \frac{2[Eu]_{SN}}{[Sm]_{SN} + [Gd]_{SN}}.$$

Due to the anomalous behavior of La in the oxidation zone, the traditional formula (2) for calculating the Ce anomaly values can lead to an overestimation of the Ce contents. Therefore, P.Joss and M.Lawrence [5] suggested using the following formula:

$$\frac{Ce_{SN}}{Ce^{*}_{SN}} = \frac{[Ce]_{SN}}{([Pr]_{SN})^2 + [Nd]_{SN}}.$$

Potential sources of manganese. One of the most important but challenging issues in the formation of manganese deposits is determining the primary source of Mn solutions. Most of the world manganese deposits are classified into four categories [1, 26, 35]:

• Sedimentary manganese deposits are a chemogenic type of ore deposits formed as precipitation from a manganese-rich solution. The source of manganese may be either the result of its dissolution during weathering of terrigenous rocks or hydrothermal solutions accompanying island-arc volcanism in the marine environment.

• Magmatogenic (hydrothermal and contact metasomatic) – hydrothermal ore deposits, which were formed because of sedimentation of manganese-rich aqueous solutions in the vicinity of volcanic vents.

• Weathering crust, residual, infiltration, etc. deposits – near-surface accumulation of manganese oxyhydroxides and oxides as a result of the manganese-bearing rocks weathering and dissolution.

• Metamorphosed deposits are formed because of regional or contact metamorphism of sedimentary or magmatic ore clusters. Usually, such deposits arise as a consequence of metamorphism of pre-existing manganese deposits of any genesis.

South Africa is known to include the giant reserves of the Paleoproterozoic sedimentary manganese ore cluster in the Kalahari region and the karst Postmasburg manganese deposit. It is necessary to pay attention to a number of ideas about the genesis of these manganese deposits in South Africa [21, 23, 42]. For example, the ore in the Kalahari deposits consists mainly of kutnahorite and braunite, i.e. from the minerals that make up the Mamatwan-type ore, and, in the zone of its secondary alterations, known as the Wessel-type ore [15, 16, 19]. The proposed ore genetic models range from the formation of manganese ores through metasomatic alteration of iron-manganese formations to chemogenic sedimentary models or volcanogenic sedimentary and transgressive-regressive mechanisms of manganese sedimentation coming from a distal volcanic source and from the underlying Ongeluk formation.

The model of manganese ore genesis of recent years is the model proposed by N.Bix et al. in 2016 [7]. In this case, the example of ore formation of the Postmasburg deposit suggests karst leaching of manganese-rich dolomites and residual accumulation of manganese wad, which subsequently underwent diagenetic alterations. The final process causes the increase in Mn content [40].

The article is published in open access under the CC BY 4.0 license

DOI: 10.31897/PMI.2021.6.4

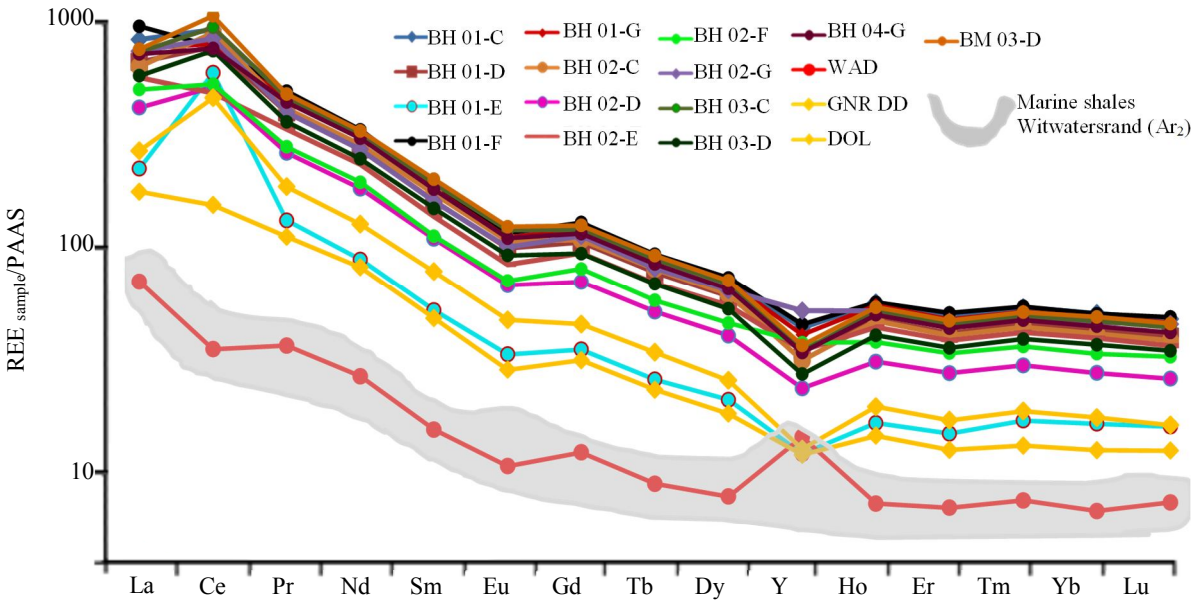


Fig.2. REE spectra in ore samples normalized on the PAAS mean values [39]

Returning to the manganese ores of the Heifeld region, it should be noted that the genesis of these deposits has also been previously discussed [27, 32, 33]. In contrast to the Kalahari and Postmasburg manganese deposits, the ore minerals here are predominantly composed of manganese oxyhydroxides: romanechite, cryptomelane, pyrolusite, lithiophorite, and vernadite. The predominance of these mineral phases and the absence of any manganese carbonates and silicates are typical signs of near-surface conditions for the accumulation of ore minerals. They were formed as a result of weathering, leaching, dissolution, and residual enrichment of pre-existing manganese-bearing rocks. The primary manganese-bearing rocks are mainly dolomites of the Malmani subgroup. These rocks contain up to 8 wt. % of MnO on average.

SEM-EDS petrographic analysis of dolomites polished sections showed the presence of manganese carbonates and silicates in small inclusions. The primary minerals here could be kutnahorite, rhodochrosite, and braunite. However, only manganese oxides were noted during the XRD study of these samples. C.Roy [35, 36] suggested that the initial presence of rhodochrosite as the primary manganese matrix, being under low temperature and intense oxidation, subsequently leads to the formation of pyrolusite and cryptomelane.

Genetic model of the Northwest manganese ore occurrence. To build a genetic model of the Northwest manganese ore occurrence, the results of analyses of the rare and rare-earth elements contents in ores, as well as petrographic, mineralogical and X-ray spectral analyses were used. The REE contents in manganese ore samples, normalized to the Post-Archean Australian shale, are shown in Fig.2. REE_{SN} in ores is characterized by relative enrichment in LREE.

$MREE_{SN}$ are slightly elevated in content over the reference with a sharp decrease and alignment of the relative concentrations in the $HREE_{SN}$ spectra (Fig.2). The REE spectra show a pronounced positive Ce_{SN} anomaly and a negative Y_{SN} anomaly. The presence of positive and negative Ce $_{SN}$ and Y $_{SN}$ anomalies, respectively, is a characteristic feature of hydrogenetic/hydrogenic mineral sediments [13, 17, 25]. These anomalies and ore enrichment with light rare-earth elements (LREE) are observed in samples with increased content of supergene minerals: cryptomelane and hollandite-romanechite.

The article is published in open access under the CC BY 4.0 license

It is important to note that the manganese wad sample (WAD), in contrast, is characterized by a positive Y and a negative Ce-anomalies, i.e., the composition of the manganese wad is closer to the composition of black coaly shale interlayers of marine origin in the underlying dolomite section. It can probably be concluded that the manganese wad was formed due to the diagenetic transformation of dolomites and coaly shale interlayers simultaneously with the formation of the Post-African I surface uplift and erosion, which preceded the formation of manganese nodules [31, 33, 43].

Using statistically substantiated genetic diagrams, it is possible to clearly distinguish ores of hydrogenous, diagenetic, and hydrothermal origin [6, 7]. The results of analyzes of samples from the Northwest ore occurrence are plotted on a ternary plot with the following vertices: Mn, Fe, and Cu + Ni + Co, and fields of compositions of ores formed under lacustrine and continental shelf conditions. K.Nicholson et al. proposed [30] a binary diagram (Co + Ni) – (As + Cu + Mo + + Pb + V + Zn), which separates the compositions of supergene and hydrothermal ores. The reliability of the conclusions, obtained from these diagrams is supported by data on the distributions of rare and rare-earth elements. It is known that manganese oxides contain a relatively high amount of RE and REE adsorbed from aqueous solutions during the precipitation of minerals. Coherent behavior of rare-earth elements in natural environments allowed S.Sun, F.McDonough [37],

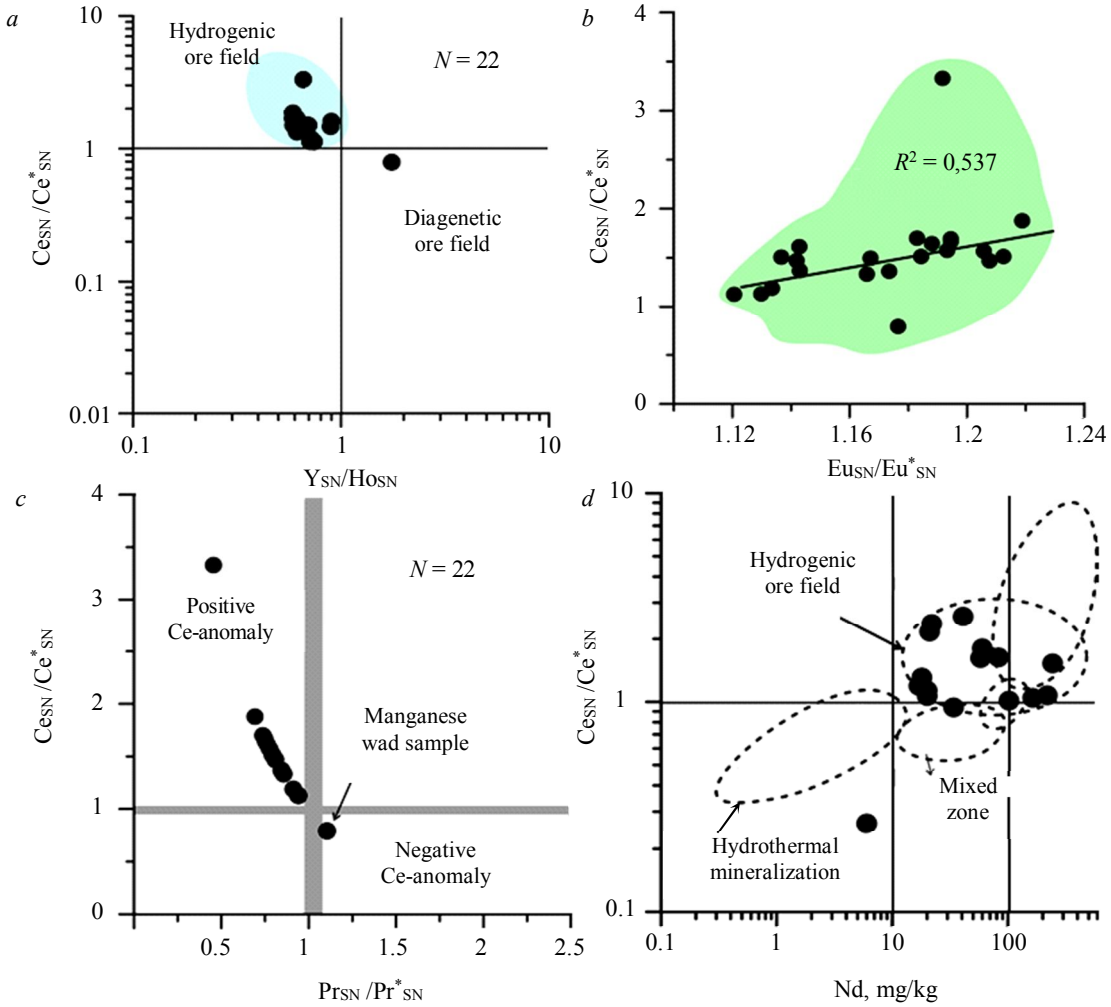


Fig.3. Supergene ore and hydrogenic Northwest manganese ore occurrence: *a* – diagram in Ce $_{SN}$/Ce*$_{SN}$-Y$_{SN}$/Ho$_{SN}$coordinates with the highlighted fields of ores of different genetic types [5, 17]; *b* – diagram in Ce -$_{SN}$/Ce*$_{SN}$-Eu$_{SN}$/Eu*$_{SN}$ coordinates shows a relatively positive correlation between Eu and Ce anomalies [5]; *c* – diagram in Ce$_{SN}$/Ce*$_{SN}$-Pr$_{SN}$/Pr*$_{SN}$ coordinates indicates the presence of strong positive Ce anomalies in the samples [6]; *d* – Ce $_{SN}$/Ce*$_{SN}$-Nd anomaly confirms hydrogenetic character of the studied samples formed during the sedimentation of ore matter from colloidal sols during leaching and dissolution of manganese dolomites [5, 13]

The article is published in open access under the CC BY 4.0 license

Journal of Mining Institute. 2021. Vol. 252. P. 814-825
DOI: 10.31897/PMI.2021.6.4
© Aleksandr N. Evdokimov, Benedict L. Pharoe, 2021

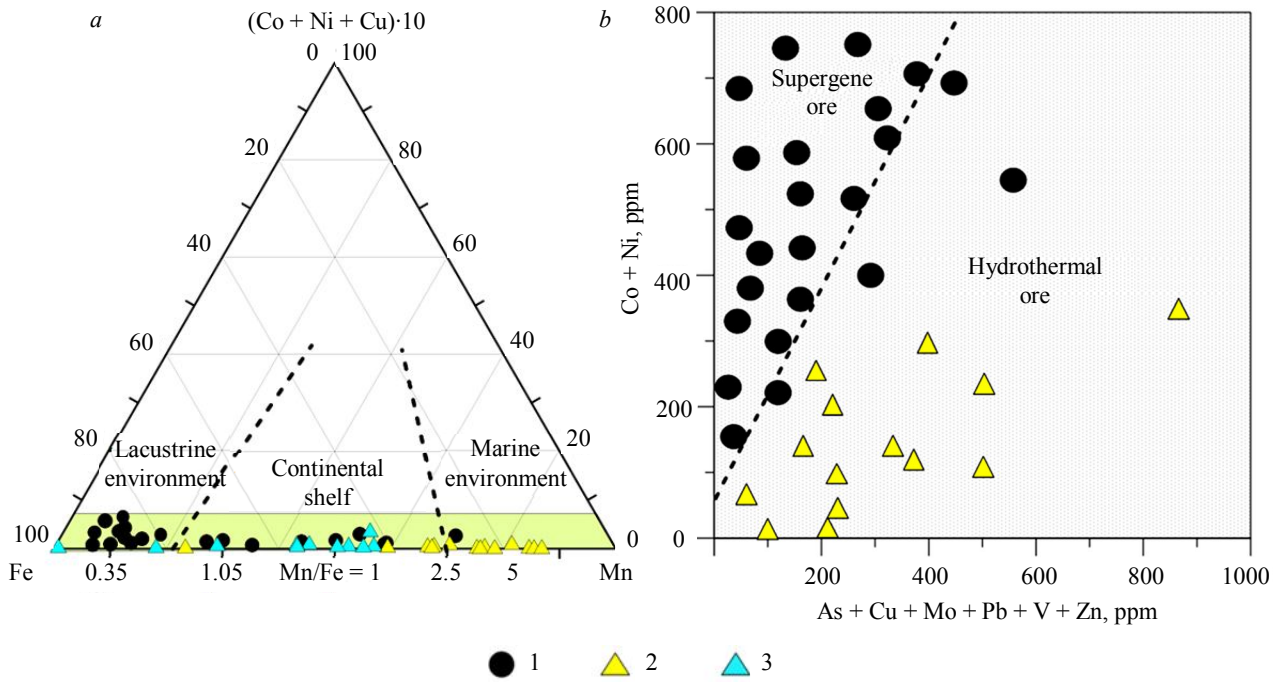


Fig.4. Diagrams of the genetic classification of manganese ore formation: the studied samples experience hydrogenetic growth from manganese-rich sols transferred in suspension from manganese-bearing dolomites in lacustrine (*a*) and supergene (*b*) settings, according to [8, 30]

1 – samples from the Northwest ore occurrence; 2 – Kalahari deposits; 3 – West Wits ore occurrences

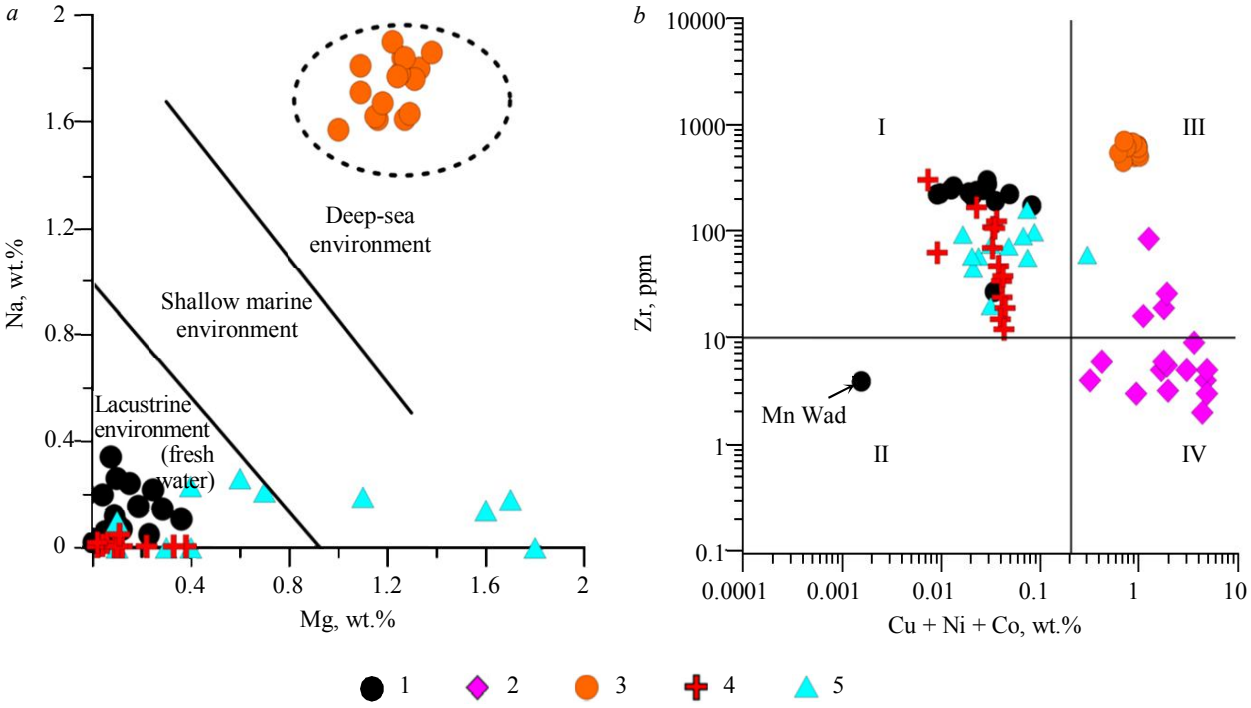


Fig.5. Genetic diagrams of manganese ore deposits: *a* – ores of the Northwest ore occurrence were formed in a lacustrine setting; *b* – have signs of hydrogenous ore formation

I – hydrogenous mineralization in the supergene zone; II – diagenetic field of mineral alterations in the oxidation zone; III – hydrogenous field of mineralization under seabed conditions; IV – hydrothermal field of mineralization under seabed conditions; 1 – samples from the Northwest ore occurrence; 2 – samples of oceanic ferromanganese nodules from the Cook Islands, according to [13]; 3 – samples from the Ryedale ore occurrence, according to [38]; 4 – samples from the West Wits manganese ore occurrence, according to [33]; 5 – samples from the Wallis and Futuna manganese deposits, according to [5]

The article is published in open access under the CC BY 4.0 license

M.Bau et al. [17], and P.Josso et al. [5] to find additional criteria for the genetic classification of ore matter, taking into account the relationship between Ce and Y anomalies and Nd concentration (Fig.3).

It should be emphasized that the compositions of ores from the Northwest ore occurrence on the ternary plot according to E.Bonnati et al. [8] are dispersed along the Fe-Mn base, which indicates the predominance of these elements and the subordinate content of Co, Ni, and Cu (Fig. 4, *a*). Hydrothermal samples from the Kalahari manganese deposit are biased toward Mn because of their lower trace element content (Co + Cu + Ni). The K.Nicholson diagram (Fig.4, *b*) [30] shows the distribution of ore compositions from the Northwest ore occurrence in the field of supergene ores, these ore samples are hydrogenetic, in accordance with the diagrams [5, 12]: the Ce_{SN}/Ce^{*}_{SN} -Y_{SN}/Ho_{SN} ratio (Fig.3, *a*); Ce_{SN}/Ce^{*}_{SN} Nd (Fig.3, *g*); Na-Mg (Fig.5, *a*); (Cu + Ni + Co)–Zr (Fig.5, *b*).

Based on the observed regularities in the distribution of rare-earth elements and ore compositions on genetic diagrams, the model of the Northwest ore occurrence can be determined as follows:

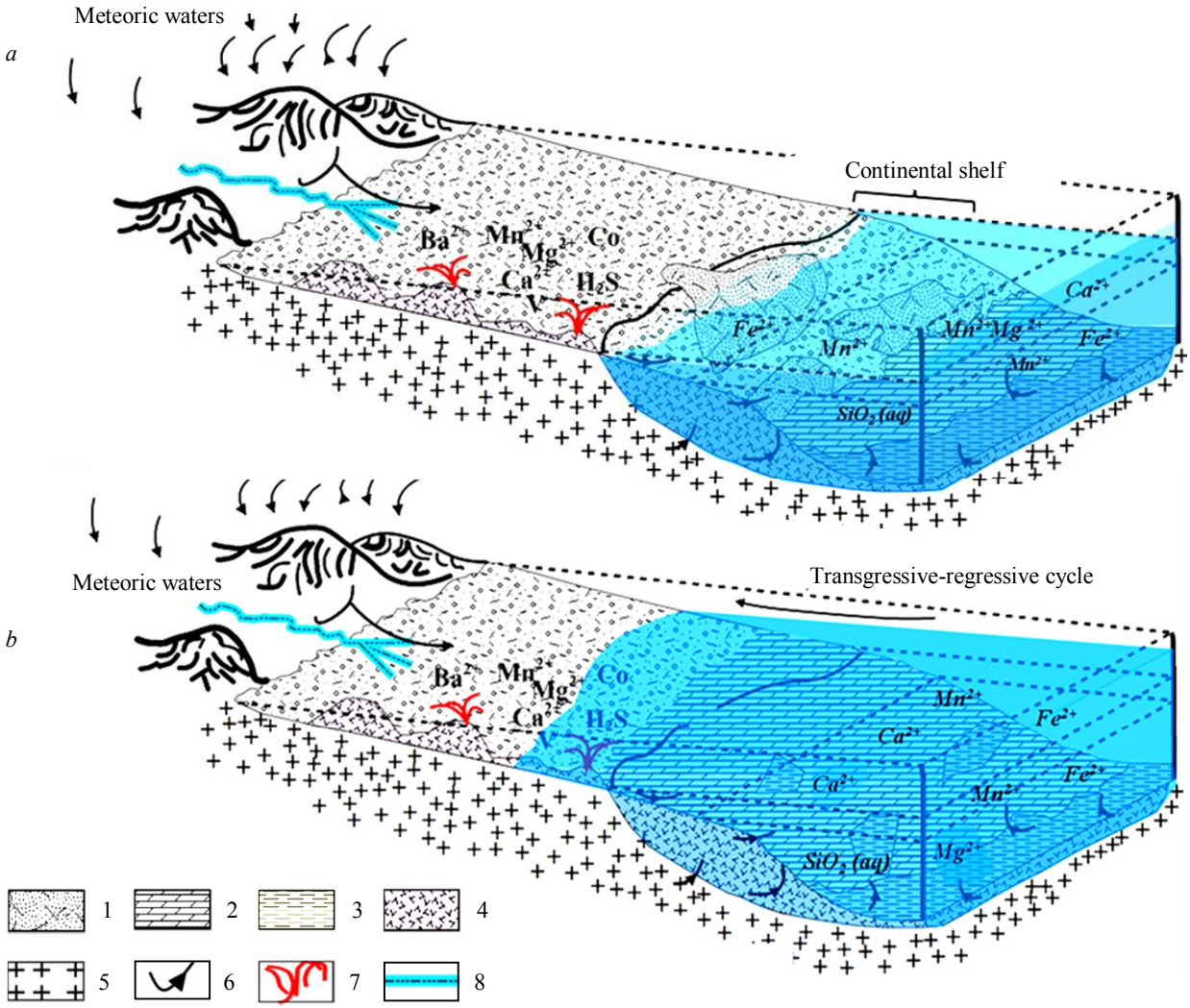


Fig.6. Initial stages of formation of the Northwest manganese ore occurrence: formation of the Malmani dolomites (*a*) and deposition of marine sediments (*b*)

1 – quartzite of the Black Reef series (Ar_1); 2 – Neoarchean Malmani dolomites (Ar_2); 3 – black coaly shale (??); (4) Ventersdorp basaltic lavas (Ar_1); 5 – granites, granite-gneisses of the Kaapvaal Craton; 6 – hydrothermal solutions associated with the previous Ventersdorp volcanic event; 7 – volcanic eruption; 8 – river systems (first, second, and fourth stages)

The article is published in open access under the CC BY 4.0 license

Journal of Mining Institute. 2021. Vol. 252. P. 814-825
DOI: 10.31897/PMI.2021.6.4
© Aleksandr N. Evdokimov, Benedict L. Pharoe, 2021

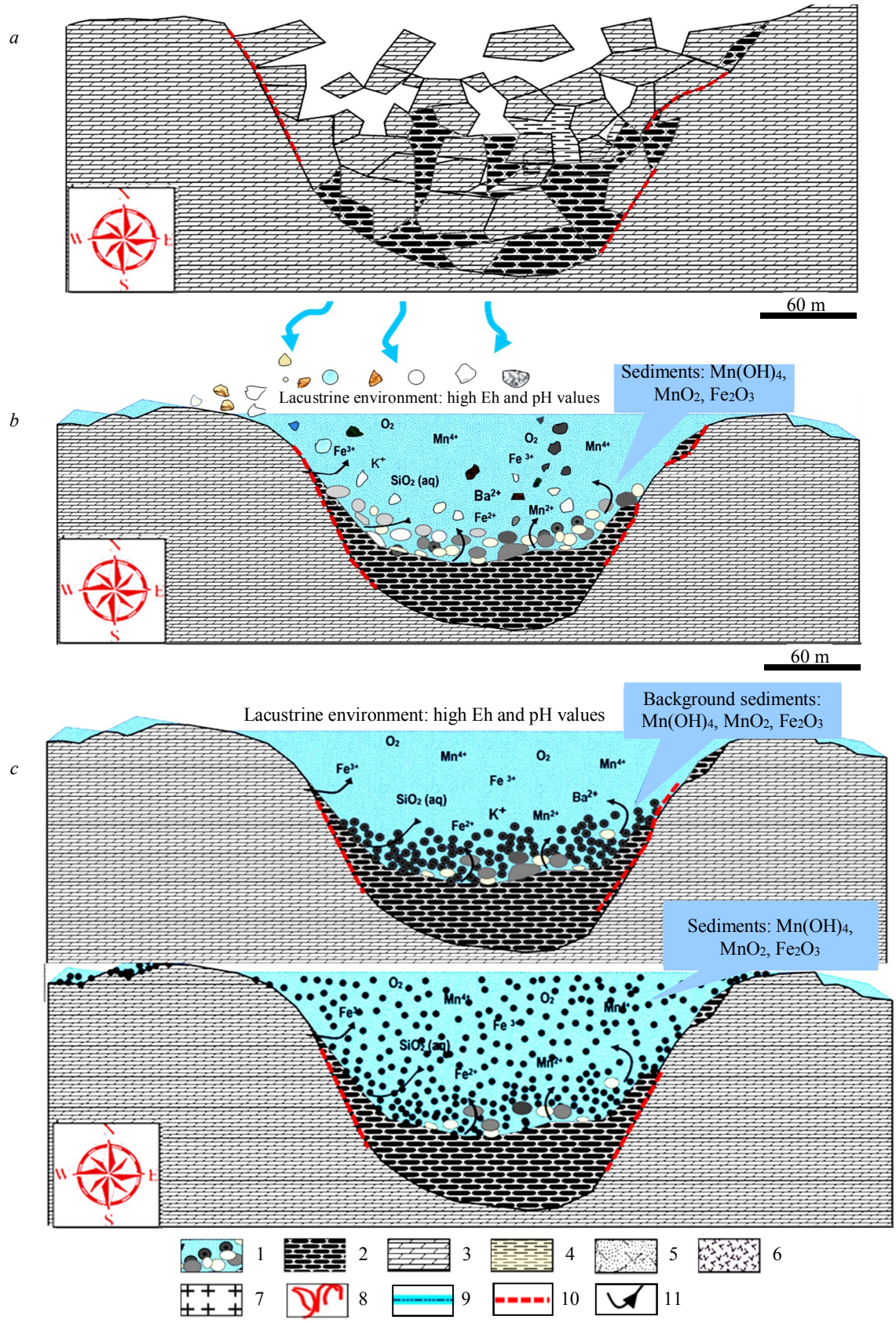


Fig.7. Formation stages of the Northwest manganese ore occurrence are: the destruction of manganese-bearing dolomites and layers of coaly black shales in the supergene zone (*a*); formation of terrigenous deposits during a sea-level fall (*b*); formation of manganese nodules (*c*)

1 – manganese nodules (N_1); 2 – manganese wad (K_2??); 3 – Neoarchean Malmani dolomites (Ar_2); 4 – black coaly shale (??); 5 – quartzite of the Black Reef series (Ar_1); 6 – Ventersdorp basaltic lavas (Ar_1); 7 – granites, granite-gneisses of the Kaapvaal craton; 8 – volcanic eruption; 9 – river systems (first, second, and fourth stages); 10 – faults; 11– hydrothermal solutions associated with the previous Ventersdorp volcanic event

The article is published in open access under the CC BY 4.0 license

• First, at the platform stage, a predominantly dolomite sequence of Neoarchean Malmani dolomites (Ar_2) was formed under marine basin conditions, enriched in manganese, magnesium, calcium, and iron cations. Oceanic aqueous solutions were probably enriched in ore from hydrothermal fluids that evaporated during the pre-Ventersdorp volcanic event (Ar_1) (2.7 Ga ago). The ore material could be also supplied due to erosion of the nearby continental land (Fig.6, *a*).

• Later, sea-level rise occurred, which led to regressive-transgressive cycles, recorded in the formation of three-layer manganese ore bodies of the Khotazelskaya suite [18, 29]. A transgressive episode of sea level movement has been documented in the Transvaal region, where the Malmani dolomites are deposited over alluvial quartz arenites of the Black Reef Formation [9, 10, 18]. During the transgressive cycle, the Malmani dolomites came onshore in the typical open Transvaal epeiric sea, which covered much of the South African landscape on the northern and western flanks of the Kaapvaal Craton (Fig.6, *b*)

• In the Late Cretaceous and Middle Cenozoic, two uplifts and erosions of the Post-African land surface were recorded [11, 31], which led to the denudation of the Malmani dolomites and coaly shales under the surface chemical weathering by meteoric waters. These erosional events are known as Post-African I and Post-African II uplift and erosion surfaces [38]. The exhumed manganese-bearing dolomites underwent a process of intense chemical weathering and dissolution, which led to the leaching of ore components (Fe, Mn, Ca, Mg, etc.) into the environment. The uplift of the territory gave rise to the formation of the Post-African I erosion surface about 77 Ma ago [43]. The formation of manganese wad began due to the destruction of coaly shales (Fig.7, *a*). This process was reflected in the sections of the ore deposit of the Northwest ore occurrence, where clay interlayers are visible in the manganese wad. XRD analysis revealed elevated contents of clay material and lithiophorite in the manganese ore. The REE spectrum (Fig.7, *b*) with a negative Ce-anomaly provides additional information on this subject. This indicates the early formation of a manganese wad on the Post-African I peneplain surface, preceding the formation of manganese nodules. The material from which the manganese wad is formed is black coaly shale of the lower Malmani subgroup.

• The formation of manganese nodules with ore matter formed due to leaching and dissolution of manganese-bearing dolomites of the Malmani subgroup in a lacustrine setting occurred during the second event – regional erosion (Fig.7, *c*). Ore components entered the overlying water column in the form of manganese colloids. This can be seen in the REE spectra, where the compositions of dolomite samples perfectly coincide with the compositions of manganese nodules (see Fig.2).

Conclusions. Indicator properties of rare and rare-earth elements in the studied manganese nodules and wad allowed restoring the sequence of formation of manganese ore deposits within the Northwest manganese ore occurrence. The data obtained on the basis of a representative volume of samples, analyzed by SEM-EDS, XRF, and ICP-MS, allowed to substantiate a genetic model of the multi-factorial process of manganese ore genesis in the Northwest province of South Africa.

In this regard, it becomes possible to use the indicator properties of rare and rare-earth elements to restore the genetic history of the new, not yet studied, manganese ore occurrences by analogy with the results obtained in this work. The properties of such indicator elements as Cu, Ni, Co, Pr, Ce, La, and highly charged Y and Zr, provide a reliable determination of manganese sources in the study of new promising deposits.

Supergene manganese deposits are characterized by the presence of manganese oxide phases, which are the products of secondary enrichment as a result of near-surface weathering and dissolution of primary manganese-bearing rocks. Like other supergene deposits, the Northwest manganese ore occurrence consists mainly of manganese oxides of the high valence state Mn^{4+}. These minerals are known for their physical and chemical properties, which make it possible to extract relatively high concentrations of rare and rare-earth elements from aqueous solutions during precipitation. The peculiarity of the geochemical behavior of these elements can be used to determine the ore source.

The article is published in open access under the CC BY 4.0 license

REFERENCES

1. Kuleshov V.N. Manganese rocks and ores: isotope geochemistry, genesis, evolution of ore genesis: Monografiya. Moscow: Nauchnyi mir, 2013, p. 508 (in Russian).

2. Tsykin R.A. Hypergene Manganese Ores of Central Siberia. *Journal of Siberian Federal University. Engineering & Technologies*. 2008. Vol. 1. N 1, p. 3-16 (in Russian).

3. Yudovich Ya.E., Ketris M.P. Manganese geochemistry in supergene processes. A review. *Biosfera*. 2013. Vol. 5. N 1, p. 21-36 (in Russian).

4. Yudovich Ya.E., Ketris M.P. Basic laws of manganese geochemistry. Syktyvkar: Komi nauchnyi tsentr Uralskogo otdeleniya Rossiiskoi akademii nauk, 2013, p. 40 (in Russian).

5. Josso P., Pelleter E., Pourret O. et al. A new Discrimination scheme for oceanic ferromanganese deposits using high field strength and rare earth elements. *Ore Geology Reviews*. 2017. Vol. 87, p. 3-15. DOI: 10.1016/j.oregeorev.2016.09.003

6. Bau M., Dulski P. Distribution of yttrium and rare-earth elements in the Penge and Kuruman iron-formations, Transvaal Supergroup, South Africa. *Precambrian Research*. 1996. Vol. 79. Iss. 1-2, p. 37-55. DOI: 10.1016/0301-9268(95)00087-9

7. Beukes N.J., Swindell E.W., Wabo H. Manganese deposits of Africa. *Episodes Journal of International Geoscience*. 2016. Vol. 39. Iss. 2. P. 285-317. DOI: 10.18814/epiiugs/2016/v39i2/95779

8. Bonatti E., Kraemer T., Rydell H. Classification and genesis of submarine iron manganese deposits. Ferromanganese Deposits of the Ocean Floor, 1972, p. 473-489.

9. Button A. The stratigraphic history of the Malmani Dolomite in the eastern and north-eastern Transvaal. *South African Journal of Geology*. 1973. Vol. 76. Iss. 3, p. 229-247. DOI: 10.10520/AJA10120750_282

10. Button A. Geochemistry of the Malmani Dolomite of the Transvaal Supergroup in the Northeastern Transvaal. *Economic Geology Research Unit*. 1975. Vol. 97, p. 1-21.

11. Burke K., Gunnell Y. The African erosion surface: a continental-scale synthesis of geomorphology, tectonics, and environmental change over the past 180 million years. *Memoir of the Geological Society of America*. 2008. Vol. 201, p. 66.

12. Bau M., Koschinsky A., Dulski P., Hein J.R. Comparison of the partitioning behaviours of yttrium, rare earth elements, and titanium between hydrogenetic marine ferromanganese crusts and seawater. *Geochimca et Cosmochima Acta*. 1996. Vol. 60. Iss. 10, p. 1709-1725. DOI: 10.1016/0016-7037(96)00063-4

13. Hein R., Spinardi F., Okamoto Mizell N. et al. Critical metals in manganese nodules from the Cook Islands EEZ, abundances and distributions. *Ore Geology Reviews*. 2015. Vol. 68, p. 97-116. DOI: 10.1016/j.oregeorev.2014.12.011

14. Deep Sea Minerals: Manganese Nodules, a physical, biological, environmental, and technical review. E.Baker, Y.Beaudoin (Editors). *SPC*. 2013. Vol. 1B. Secretariat of the Pacific Community, p. 51.

15. de Villiers J. The manganese deposits of the Union of South Africa. Geological Survey of South Africa Handbook 2. Pretoria: Government Printer, 1960, p. 263.

16. de Villiers P. The geology and mineralogy of the Kalahari Manganese Field north of Sishen, Cape Province. Pretoria: Geological Survey of South Africa, Memoir 59, 1970, p. 84.

17. Bau M., Schimdt K., Koschinsky A. et al. Discriminating between different genetic types of marine ferro-manganese crusts and nodules based on rare earth elements and yttrium. *Chemical Geology*. 2014. Vol. 381, p. 1-9. DOI: 10.1016/j.chemgeo.2014.05.004

18. Eriksson K. Cyclic sedimentation in the Malmani Dolomite, Potchefstroom Synclinorium. *Geological Society of South Africa*. 1972. Vol. 75. Iss. 2, p. 85-97. DOI: 10520/AJA10120750_2731

19. Frankel J. Manganese ores from the Kuruman district, Cape Province, South Africa. *Economic Geology*. 1958. Vol. 53, p. 577-597. DOI: 10.2113/gsecongeo.53.5.577

20. Del Rio Salas R., Ruiz J., Ochoa-Landin L. et al. Geochemistry and Re-Os systematics of manganese deposits from the Santa Rosalia Basin and adjacent area in Baja California Sur, Mexico. *Mineralium Deposita*. 2008. Vol. 43. Iss. 4, p. 467-482. DOI: 10.1007/s00126-008-0177-3

21. Gutzmer, J. Genesis and alteration of the Kalahari and Postmasburg Manganese Deposits, Griqualand West, South Africa: PhD dissertation, University of Johannesburg. South Africa, 1996, p. 490.

22. Heshmatbehzadi K., Shahabpour J. Metallogeny of manganese and ferromanganese ores in Baft Ophiolitic Mélange, Kerman, Iran. *Australian Journal of Basic and Applied Sciences*. 2010. Vol. 4. Iss. 2, p. 302-313.

23. Kleyenstuber A. The mineralogy of the manganese bearing Hotazel Formation of the Proterozoic Transvaal Sequence in Griqualand West, South Africa. *Transactions of the Geological Society of South Africa*. 1984. Vol. 87. Iss. 3, p. 257-272.

24. Achurra L.E., Lacassie J.P., Le Roux J.P. et al. Manganese nodules in the Miocene Bahia Inglesa Formation, north-central Chile: Petrography, geochemistry, genesis and palaeoceanographic significance. *Sedimentary geology*. 2009. Vol. 217. Iss. 1-4, p. 128-139. DOI: 10.1016/j.sedgeo.2009.03.016

25. Garnit H., Kraemer D., Bouhlel S. et al. Manganese ores in Tunisia: Genetic constraints from trace element geochemistry and mineralogy. *Ore Geology Reviews*. 2020. Vol. 120. N 103451. DOI: 10.1016/j.oregeorev.2020.103451

26. Maynard J.B. The chemistry of manganese ores through time: a signal of increasing diversity of earth-surface environments. *Economic Geology*. 2010. Vol. 105. Iss. 3, p. 535-552. DOI: 10.2113/gsecongeo.105.3.535

27. Pharoe B.K., Evdokimov A.N., Gembitskaya I.M., Bushuev Y.Y. Mineralogy, geochemistry and genesis of the post-Gondwana supergene manganese deposit of the Carletonville-Ventersdorp area, North West Province, South Africa. *Ore Geology Reviews*. 2020. Vol. 120. N 103372. DOI: 10.1016/j.oregeorev.2020.103372

28. Nath B.B. Nath B.B., Pluger W.L., Roelandts I. Geochemical constraints on the hydrothermal origin of ferromanganese incrustations from the Rodriguez triple junction, Indian Ocean. *Geological Society of London, Special Publication*. 1997. Vol. 119, p. 199-211. DOI: 10.1144/GSL.SP.1997.119.01.13

29. Nel C., Beukes N., De Villiers J. The Mamatwan manganese mine of the Kalahari manganese Field. *Mineral Deposits of Southern Africa. Geological Society of South Africa*. 1986. Vol. 1, p. 963-978.

The article is published in open access under the CC BY 4.0 license

30. Nicholson K., Nayak V.K., Nanda J.K. Manganese ores of the Ghoriajhor-Monmunda area, Sundergarh District, Orissa, India: geochemical evidence for a mixed Mn source. *Geological Society of London, Special Publication*. 1997. Vol. 119. Iss. 1, p. 117-121. DOI: 10.1144/GSL.SP.1997.119.01.08

31. Partridge T.C., Maud R.R. Geomorphic evolution of Southern Africa since Mesozoic. *South African Journal of Geology*. 1987. Vol. 90. Iss. 2, p. 179-208. DOI: 10520/AJA10120750_958

32. Pharoe B.K., Liu K. Stratigraphy of the pedogenic manganese nodules in the Carletonville area, North West Province of South Africa: A case study of the General Nice Manganese Mine. *Journal of African Earth Sciences*. 2018. Vol. 143, p. 79-101. DOI: 10.1016/j.jafrearsci.2018.03.002

33. van Niekerk H.S., Beukes N.J., Gutzmer J. Post-Gondwana pedogenic ferromanganese deposits, ancient soil profiles, African land surfaces and palaeoclimate change on the Highveld of South Africa. *Journal of African Earth Sciences*. 1999. Vol. 29. Iss. 4, p. 761-781. DOI: 10.1016/S0899-5362(99)00128-1

34. Yi Zhong, Zhong Chen, Francisco Javier Gonzalez et al. Rare earth elements and yttrium in ferromanganese deposits from the South China Sea: distribution, composition and resource considerations. *Acta Oceanologica Sinic*. 2019. Vol. 37. Iss. 7, p. 41-54. DOI: 10.1007/s13131-018-1205-5

35. Roy S. Environments and processes of manganese deposits. *Economic Geology*. 1992. Vol. 87. N 5, p. 1218-1236. DOI: 10.2113/gsecongeo.87.5.1218

36. Roy S. Sedimentary manganese metallogenesis in response to the evolution of the Earth system. *Earth Science reviews*. 2006. Vol. 77. Iss. 4, p. 273-305. DOI: 10.1016/j.earscirev.2006.03.004

37. Sun S., McDonough W. Chemical and isotopic systematics of oceanic basalts: implications for mantle composition and processes. *Geological Society of London*. 1989. Vol. 42, p. 313-345. DOI: 10.1144/GSL.SP.1989.042.01.19

38. Pack A., Gutzmer J., Beukes N., Van Niekerk H. Supergene ferromanganese wad deposits derived from Permian Karoo Strata along the late Cretaceous-mid-Tertiary African land surface, Ryedale, South Africa. *Economic Geology*. 2000. Vol. 95. N 1, p. 203-220. DOI: 10.2113/gsecongeo.95.1.203

39. Taylor S.R., Mclennan S.M. The Continental Crust: Its Composition and Evolution. Oxford: Blackwell Scientific, 1985, p. 312.

40. Fairey J., Timmerman J., Sudo M., Tsikos H. The Role of Hydrothermal Activity in the Formation of Karst-Hosted Manganese Deposits of the Postmasburg Mn Field, Northern Cape Province, South Africa. *Minerals*. 2019. Vol. 9. Iss. 7. N 408. DOI: 10.3390/min9070408

41. Toth J. Deposition of submarine crusts rich in manganese and iron. *Geological Society of America Bulletin*. 1980. Vol. 91. Iss. 1, p. 44-54. DOI: 10.1130/0016-7606(1980)91<44:DOSCRI>2.0.CO;2

42. Tsikos H. Petrographic and geochemical constraints on the origin and post-depositional history of the Hotazel Iron-Manganese Deposits, Kalahari Manganese Field, South Africa: PhD dissertation. Rhodes University, South Africa, 1999, p. 292.

43. Vafeas N.A., Blignaut L.C., Viljoenm K.S. New evidence for the early onset of supergene alteration along the Kalahari unconformity. *South African Journal of Geology*. 2018. Vol. 121. N 2, p. 157-170. DOI: 10.25131/sajg.121.0012

44. Varentsov I.M. Manganese Ores of Supergene Zone: Geochemistry of Formation. Springer, 1996. Vol. 8, p. 302. DOI: 10.1007/978-94-017-2174-5

***Authors*: Aleksandr N. Evdokimov,** *Doctor of Geological and Mineralogical Sciences, Professor, https//orcid.org/0000-0002-8121-0426* (*Saint Petersburg Mining University, Saint Petersburg, Russia*), **Benedict L. Pharoe,** *Postgraduate Student, benedictpharoe1@gmail.com, https//orcid.org/0000-0001-7922-9112* (*Saint Petersburg Mining University, Saint Petersburg, Russia*).

The authors declare no conflict of interests.

The article is published in open access under the CC BY 4.0 license